



Analysis of Feed through Cancellation in Hybrid MEMS Resonator

1.S.Ezhilarasan 2. C.Yuvaraj 3.K.Vijayakumar

1, 2 & 3 Assistant professor, Ganathipathy Tulsi's Jain Engineering College, Vellore.

Mail id: ezhilarasan_eee@gtec.ac.in & yuvaraj_eee@gtec.ac.in & vijayakumar_eee@gtec.ac.in

ARTICLE INFO

Article History:

Received 29th Oct, 2015

Received in revised form 1st Nov 2015

Accepted 3rd Nov, 2015

Published online 4th Nov, 2015

Keywords:

Cancellation, CMRR, MEMS, SE mode resonator, COMSOL Multiphysics.

ABSTRACT

This paper describes about Micro electromechanical systems (MEMS) resonators typically exhibit large parasitic feed through where the input drive signal is directly coupled to the output ports, presenting a challenge to full electrical characterization of resonators where the output is heavily embedded in feed through. We here present an on-chip solution that significantly mitigates the undesirable effects of parasitic feed through but using only a single device. We have demonstrated its use in a symmetrical mode of vibration (the extensional mode of a square-plate MEMS resonator) to show its applicability to most generic resonator mode shapes. In our measurements, we show that the proposed method for feed through cancellation provides a 40-dB common-mode rejection compared to when no feed through cancellation is implemented. The necessary matching of drive circuit capacitances is achieved by properly sizing and placing a dummy pad in the vicinity of each drive pad. The studies reported herein demonstrate that the integrity of the output signal from a MEMS resonator is not only determined by device dimensions but also strongly influenced by the interaction between fringing fields radiating from electrodes in proximity. These results could open up a new avenue in the design of hybrid MEMS resonant devices where the issue of feed through can be both effectively and cheaply addressed.

I. INTRODUCTION

MEMS resonators have received much interest recently as an attractive candidate to replace quartz crystals due to their small form factor and potential integration with CMOS ICs. As these mechanical devices are scaled down to the micrometer and nanometer scales, substantial reductions in size and power can be achieved, an attractive feature for portable applications. These MEMS resonators can be seen as building blocks for a larger system, functioning as precision timing elements. Such types of miniaturized timing/frequency references of themselves have been of great interest in the area of portable low-power mobile wireless communication systems [1]. For example, RF MEMS filters could be realized by physically coupling multiple MEMS resonators together, such as mechanically coupling two wine-glass-mode disk resonators through a

beam as described in [2]. Such a micromechanical filter possesses numerous benefits such as CMOS integration, small form factor, and implementation of multiple frequencies on a single chip. These present a highly attractive alternative to macro scale discrete off-chip quartz crystals and surface acoustic wave filters, promising great impact on the mobile communications industry.

MEMS resonators also hold applications to precision sensing. Resonant sensors monitor changes in the environment through detecting a shift in the resonant frequency of the MEMS device in response to the application of a desired external stimulus [3]. Resonant accelerometers are an excellent example of this class of sensors [4].

For sensing applications, the resonator could also function simply as an oscillating shuttle like in MEMS gyroscopes. Industrial applications of MEMS gyroscopes include roll-over detection in automobiles, stabilization for image recording, and GPS-assisted navigation for spacecraft [5]. As another example, the electric field sensor described in [6] is also based on a resonant shuttle and has been applied to measure dc and ac fields associated with power systems abundant in industrial applications.

II. THEORY OF RESONATOR

As Micromechanical resonators evolve to become smaller in order to achieve higher frequencies of operation, the parasitic feed through becomes more substantial compared to the large motional impedances typical which are further augmented in the process of miniaturization. Feed through is caused by the direct coupling between the drive and sense electrodes through a parasitic capacitor lying in parallel to the resonator. The resonator may be modelled by an equivalent circuit as depicted in figure shown below. C_f represents the feed through Capacitance, R_m , L_m , and C_m respectively denote the motional resistance, inductance and capacitance when a DC bias voltage is applied to the device.

One way of reducing the effects of feed through is by adopting a fully differential transduction configuration. The major limitation of this approach is that it requires a differential mechanical mode of vibration[7]. Compared to a one-port configuration, only half of all electrodes are used for actuation while the other half are reserved for sensing.

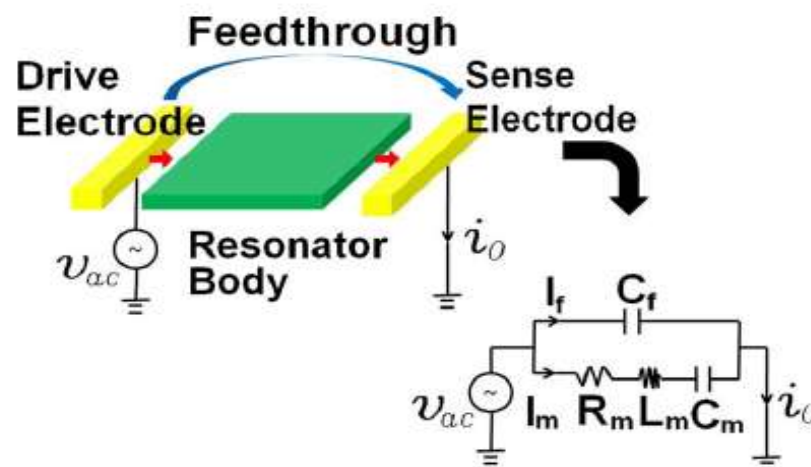


Figure.1. Electrical characterization of a MEMS resonator and its equivalent circuit .

Hence feedthrough can be substantially reduced using a fully differential transduction configuration if the device resonates in an anti symmetrical mode shape.

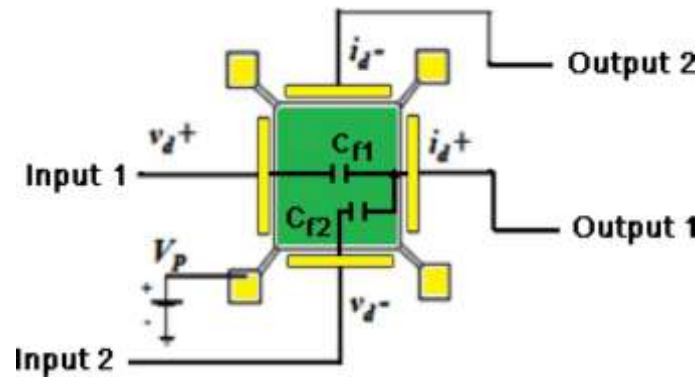


Figure.2. Feed through cancellation using differential drive.

The above figure 2 shows a square-plate resonator with electrodes on each side for electrostatic actuation and detection. The capacitors C_{f1} and C_{f2} represent the parasitic feed through path between the respective input electrodes and one of the output electrodes. By keeping the drive voltage at input 1 out of phase in relation to input 2, in the limit where the parasitic feed through capacitors C_{f1} and C_{f2} are well matched, substantial rejection of feed through at the output is achieved. By summing both outputs 1 and 2 differentially, have reported a fully differential setup that is supposed to further cancel feed through. Hence, in the fully differential setup, both the drive and sense ports are interfaced differentially. By subtracting the feed through component from the measured electrical transmission, we can obtain the mechanical resonance.

III. SQUARE WINE GLASS MODE OF RESONATOR

The square wine glass resonant mode (SWG) may be described as a square plate that contracts along one axis in the plane of fabrication, while also simultaneously extending along an orthogonal axis in the same plane, as shown in Fig.3. Since the mode shape is isochoric, losses due thermo elastic dissipation are minimized. The resonant structure is supported at each corner by T-shaped stems that connect it to the respective anchors as may be seen from the optical micrograph of the fabricated device.

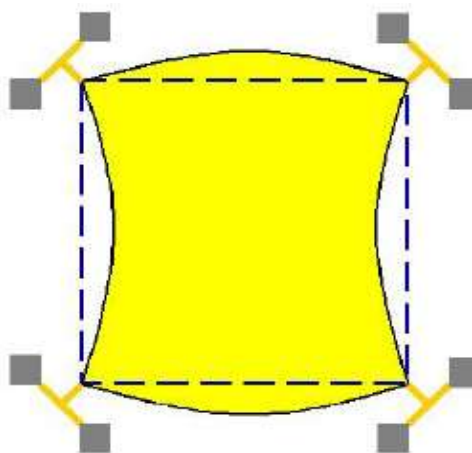


Figure 3. Illustration of the square wine glass resonant mode shape

The square structure has been excited into the anti symmetrical SWG mode by applying equal and opposite polarity DC voltages and the same AC voltage to the drive electrodes along each of the two axes(8). This results in an electrostatic force that is equal in magnitude and opposite in phase along the two in-plane orthogonal axes (x and y).

The motion of the structure is sensed through a motional current resulting from changes in the transduction gap as the structure is driven into resonance. In both cases of the LE- and SE-mode resonators, the supporting tethers are subjected to axial stress as the resonator expands/contracts and can thus be exploited as piezo resistors already built into the resonator. In both cases of the LE- and SE-mode resonators, the supporting tethers are subjected to axial stress as the resonator expands/contracts and can thus be exploited as piezoresistors already built into the resonator. Applying a dc voltage across the tethers (Vd) results in a modulated current associated with the mechanical resonance

IV. MATHEMATICAL RELATIONS

The resonator equivalent circuit parameters are given by

$$L_m = \frac{M}{\epsilon_t^2 V_P^2} \quad (1)$$

$$R_m = \frac{\sqrt{KM}}{\epsilon_t^2 V_P^2} \quad (2)$$

$$C_m = \frac{\epsilon_t^2 V_P^2}{K} \quad (3)$$

In this case, C_f represents the parasitic feed through capacitance located across the input and output ports in parallel to the series resonant tank where R_m , L_m , and C_m denote the motional resistance, inductance, and capacitance, respectively. The overall admittance can thus be expressed as

$$Y(\omega) = j\omega C_f + \frac{j\omega C_m}{[1 - (\frac{\omega}{\omega_0})^2 + j(\frac{\omega}{\omega_0})Q]} \quad (4)$$

Where ω_0 is the mechanical resonant frequency of the resonator and Q is the quality factor.

IV. EQUIVALENT CIRCUIT OF RESONATOR CIRCUIT

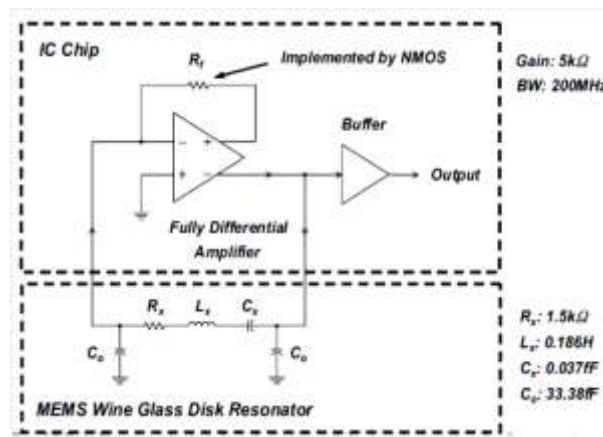


Figure. 4 Electrical Equivalent Circuit of Resonator Circuit

The resonant frequency (f_0) of a structure for a given mode of vibration is determined by its effective spring constant (k_R) and dynamic mass (M_R) is given by

$$f_0 = \frac{1}{2\pi} \sqrt{\frac{k_R}{M_R}}$$

The square wine glass resonant mode (SWG) may be described as a square plate that contracts along one axis in the plane of fabrication, while also simultaneously extending along an orthogonal axis in the same plane. The corners are stationary points, while displacement is maximum midway along the edges which bend either inwards or outwards.

The compensation capacitor in the equivalent circuit is tuned to closely match the parallel feed through capacitor. The output currents from the compensation capacitor and feed through capacitor are out of phase and hence effective cancellation of the parasitic feed through is achieved when these currents are added at the input of the trans impedance amplifier. This increases the ratio of the sensed motional current to that from the feed through capacitor, thus satisfying the condition for oscillation.

V. FULLY DIFFERENTIAL CONFIGURATION WITH ANTISYMMETRICAL MODE SHAPE

Feed through can be substantially reduced using a fully differential transduction configuration if the device resonates in an anti symmetrical mode shape, such as the wine-glass mode (9). It shows that square-plate resonator with electrodes on each side for electrostatic actuation and detection. The capacitors C_{f1} and C_{f2} represent the parasitic feed through path between the respective input electrodes and one of the output electrodes (output 1 in this case). By keeping the drive voltage at input 1 out of phase in relation to input 2, in the limit where the parasitic feed through capacitors C_{f1} and C_{f2} are well matched, substantial rejection of feed through at the output is achieved.

By summing both outputs 1 and 2 differentially have reported a fully differential setup that is supposed to further cancel feed through. Hence, in the fully differential setup, both the drive and sense ports are interfaced differentially. The fabricated SOI square-plate resonator was packaged and wire bonded in a 28-pin dual in-line chip carrier, which was mounted on a printed circuit board for full electrical characterization. The transmission characteristic of the resonator was measured under moderate vacuum (0.2 mbar) within a custom built vacuum chamber using an Agilent E5061A network analyzer. The measured transmission is given in Fig. 5, which shows a clear resonance peak.

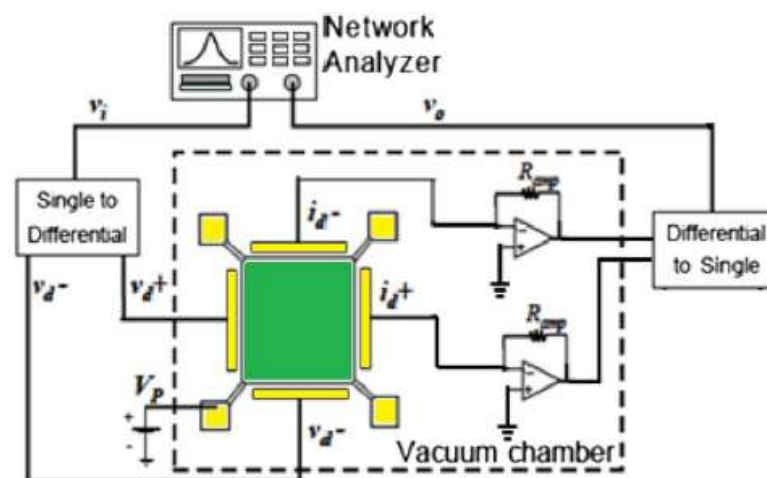


Figure.5 Fully differential configuration

The measured transmission is given in Fig. 5, which shows a clear resonance peak. From (1), it may be seen that C_m will be zero when the applied dc bias (VP) is zero, reducing the overall admittance calculated from (2) to be $j\omega C_f$. This suggests that the feed through component can be measured by simply turning off VP . The feed through, measured as such, is also shown in Fig. 5. By subtracting the feed through component from the measured electrical transmission, we can obtain the mechanical resonance as shown in Fig. 6. From the extracted curve in Fig. 5, the Q of the wine-glass-mode resonator was found to be 1.27×10^6 with a resonant frequency of 11.5MHz.

Next, the respective feed through levels were measured for the single-ended setup, as well as the fully differential setup without the amplification circuit. In addition, the output current from each sense electrode was monitored individually to assess the impact of employing a differential output relative to the differential input alone.

From the individual outputs of each sense electrode in Fig. 5, it may be seen that feed through rejection was achieved most via the differential drive (-47 dB relative to a single-ended drive input), while differential sensing at the output ports provided only an additional 10 to 12 dB reduction [17]. In short, the use of differential sense provided only marginal improvement in terms of feed through rejection compared to differential drive alone.

Two resonators of different thicknesses (10mm and 25mm) but same designed lateral dimensions were interrogated using the single-ended setup in Fig 5, and the fully differential setup depicted in Fig 4. The resonators were measured in a custom built vacuum chamber at a pressure of 0.2 mbar to reduce viscous damping on the resonator. The resonators have been electrically interrogated in the single-end configuration (Fig 5) followed by the fully-differential setup. No resonant peak was observed for the single-ended configuration. In the fully differential case, the sensed output current from each sense electrode was amplified via two trans impedance amplifiers each with a trans impedance gain of 7.5 db(10).

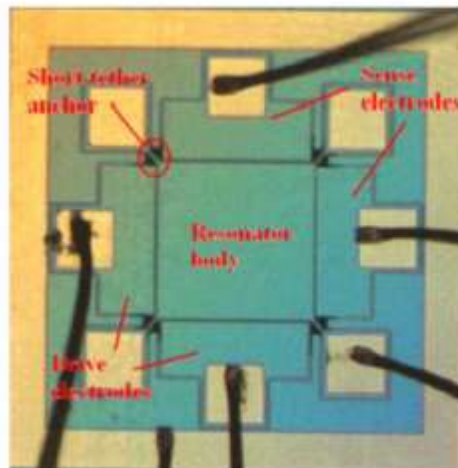


Figure.6. Optical micrograph of the square-plate resonator with electrodes

The actual motional signal without feed through can be obtained by subtracting the measured feed through signal from the overall signal, as shown in Fig 6. The value of Q may be deduced by taking the ratio of resonant frequency to the -3 dB bandwidth and was found to be 1.23×10^6 . It is worth noting that this value of Q was found to be the same as that obtained prior to de-embedding, indicative of the low feed through achieved using a fully-differential configuration.

The same measurements were conducted for the 10 mm thick square-plate resonator. Its measured transmission as a function of the applied DC bias is given in Fig 6, which shows that the decrease in thickness gives a reduction in performance relative to the 25 mm thick device. For example, the measured peak height 7.25 dB above the feed through level for the 10 mm device as compared to 16.8 dB for the 25 mm. After de embedding the feed through signal, the Q for the 10 mm device was found to be 7.4970×10^5 . Both the drop in Q and electromechanical coupling due to a reduction in the capacitive transduction area all lead to an increase in R_m for the 10 mm device. This effect of this increase in R_m can be seen from the presence of a large anti-

resonance highlighted by the circle in Fig 6. The peak value likewise drops accordingly with V_p due to a reduction in the electro-mechanical coupling. The value of Q may be deduced by taking the ratio of resonant frequency to the -3dB bandwidth and was found to be 1.23×10^6 . It is worth noting that this value of Q was found to be the same as that obtained prior to de-embedding, indicative of the low feed through achieved using a fully-differential configuration.

VI. RESULT AND DISCUSSIONS

The MEMS switch is designed using commercial software packages CMOSOL Multiphysics and Intellisuite.

TABLE1. Design parameters of MEMS resonator

PARAMETER	UNITS	SYMBOL	VALUE
Thickness of resonant structure	μm	h	25
Resonator side length	μm	L	2000
Frequency of the square wine glass resonant mode	MHz	f_0	2.006
Transduction gap	μm	G	2
Drive electrode length	μm	le	1880
Normalized transduction coefficient	nF/m	ϵ_s	104

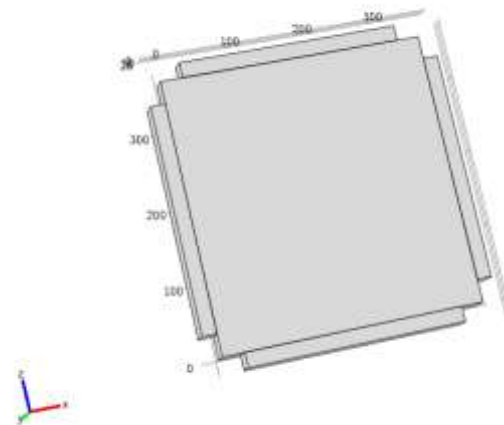


Fig.7. Resonator structure with no applied voltage.

When minimum voltage is applied to the electrodes, it behaves like an ordinary RLC resonant circuit. But the voltage is increased, the resonant peak is decreased due to the effect of feed through problem.

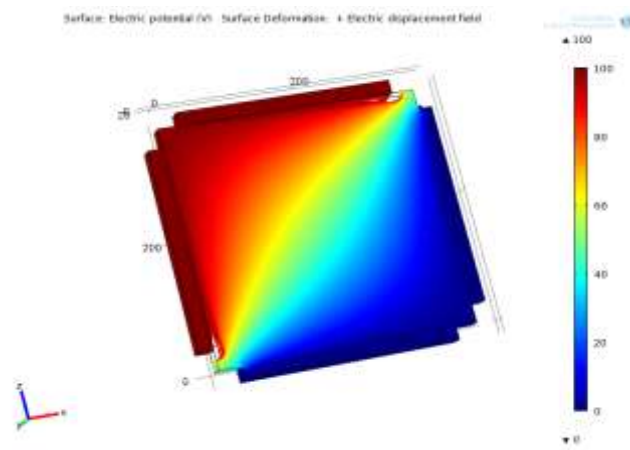


Fig.5. Resonator structure with applied voltage.

First the resonator is designed with the help of comsol using the parameters and dimensions given in Table 1. The value of Q may be deduced by taking the ratio of resonant frequency to the -3dB bandwidth and was found to be 1.23×10^6 . It is worth noting that this value of Q was found to be the same as that obtained prior to de-embedding, indicative of the low feed through achieved using a fully-differential configuration.

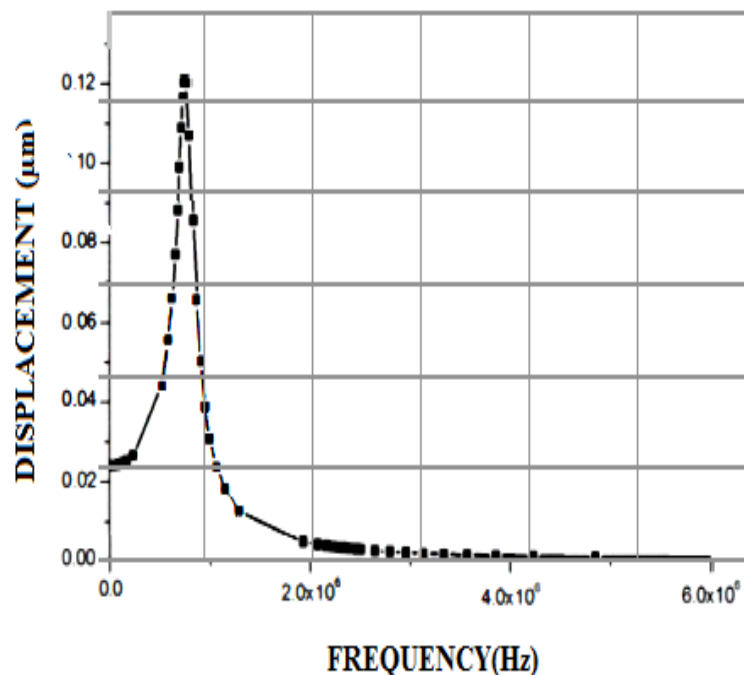


Fig.8. Graph between Frequency and displacement.

The frequency response of the resonator is obtained by a frequency sweep, in the resonance neighbourhoods of the theoretically calculated values. Theoretical calculation of resonant frequency using Eq. 5 is 0.7375 MHz. The resonant frequency is determined from the above graph of displacement as a function of frequency as well. Fig. 3.3 shows the resonant frequency 0.751 MHz along with maximum displacement of 0.12 μm in the centre of resonator structure. This small difference in resonant frequency is due to large size of meshes during Finite Element Analysis (FEM).

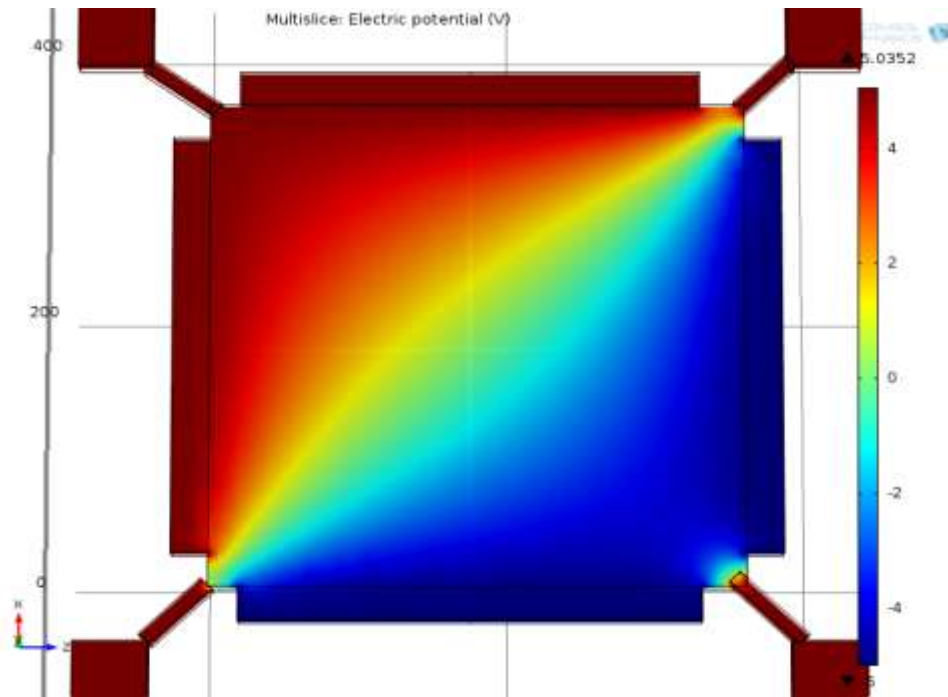


Fig.9 DIFFERENTIAL INPUT MODE OF RESONATOR.

It is obtained with different voltage is applied to the tethers. It will increase the ratio of differential voltage gain to common mode voltage gain(CMRR).

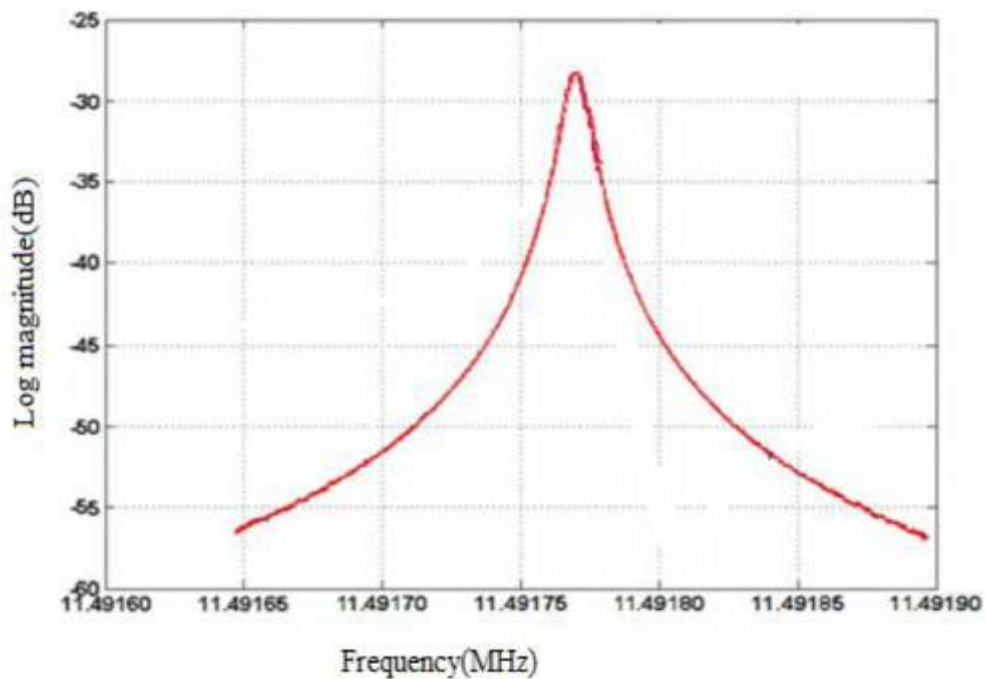


Fig.10.Determination of frequency with differential mode resonator

From the graph it is found that the peak frequency value is obtained from the log magnitude value of CMRR. The actual motional signal with feed through can be obtained by simply giving opposite polarity of dc bias voltage to the electrodes . The log magnitude value is measured by common mode rejection ratio of the resonator. The CMRR is the ratio of differential mode signal (A_d) to the common mode signal (A_c).

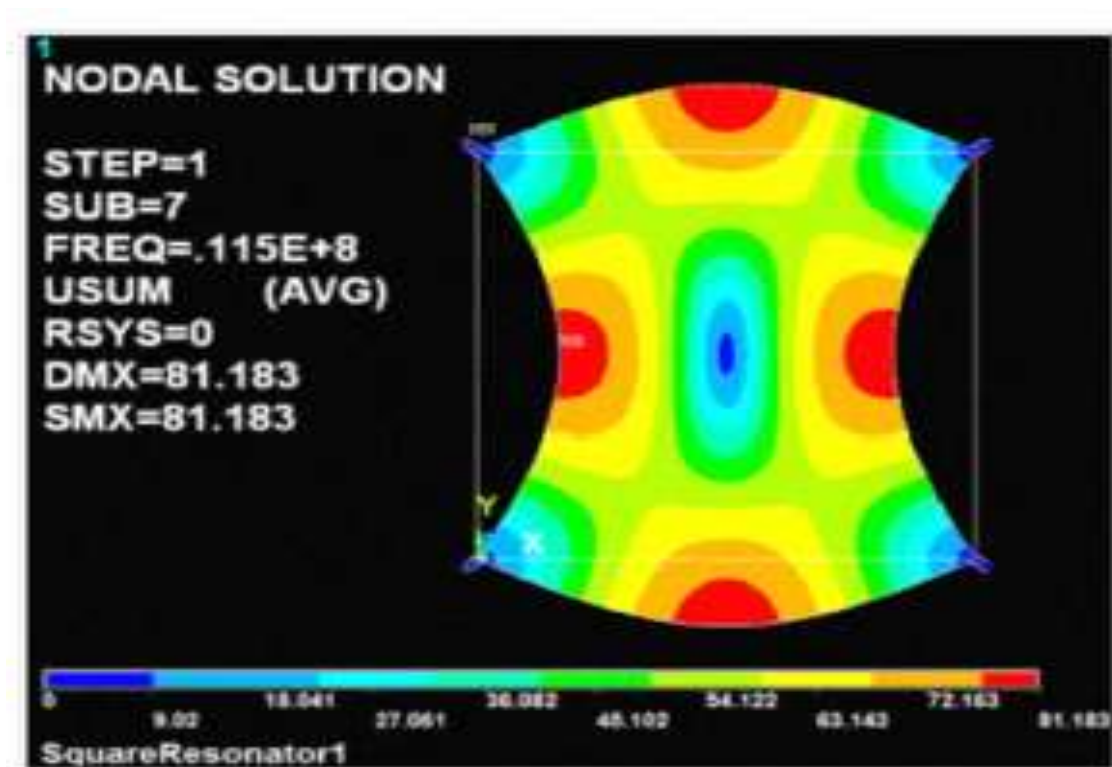


Figure.11. Simulation of the wine-glass mode using COMSOL Multiphysics.

In the fully differential case, the sensed output current from each sense electrode was amplified via two trans impedance amplifiers each with a trans impedance gain of 7.5 db. The output from each amplifier is fed into an 1800 out-of-phase input power combiner whose output in turn is monitored by the network analyzer.

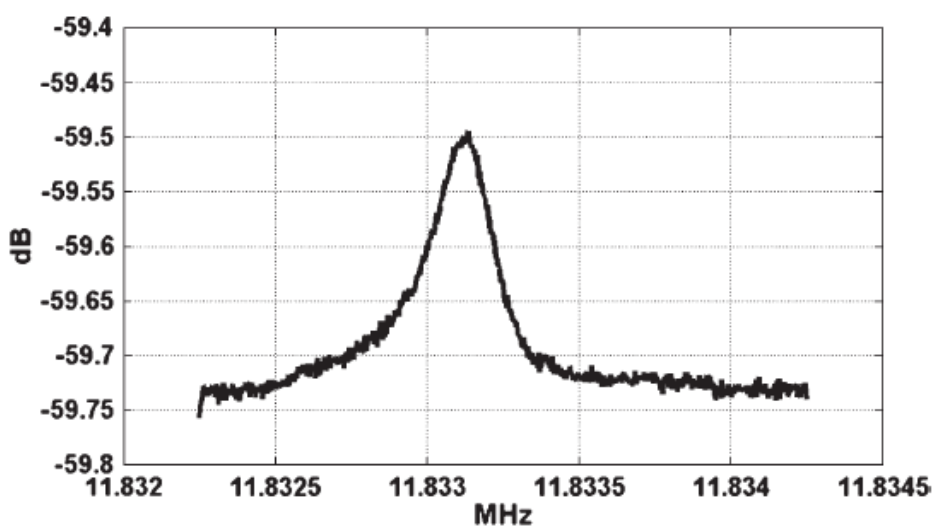


Figure.12. Graph between gain and frequency

Finally from the above graph, it is found that original resonant frequency with the presence of feed through effect.

VII. CONCLUSION

we have demonstrated in this work that hybrid MEMS resonator with structure of 10 μ m and 25 μ m exhibits a frequency of only 6-11 MHz. It is reduced due to the presence of feed through effect in resonator circuit. The effect of feed through is analysed by common mode voltage involve in frequency response of resonator circuit. also shown that in a fully-differential setup, which comprises the stages of both differential drive and differential sensing, it is the former that provides most of the common-mode feed through rejection. Hence while differential sensing can further cancel common-mode feed through, it is not as critical for resonator topologies where differential sensing is difficult to implement as opposed to differential drive.

REFERENCES

- [1] C. T.-c. Nguyen, "Transceiver front-end architectures using vibrating micromechanical signal processors," chapter in *RF Technologies for Low Power Wireless Communications*, edited by G. I. Haddad, T. Itoh, and J. Harvey, pp. 411-461. New York: Wiley IEEE-Press, 2001.
- [2] G. Stemme, "Silicon resonant sensors," *1. Micromech. Microeng.*, volume , no 2, pp 113-125,1991.
- [3] T. P. Burg et al, "Weighing of biomolecules, single cells and single nano particles in fluid," *Nature*, volume 446, pp 1066-1069, Apr 2007.
- [4] I. E.-Y. Lee and A. A. Seshia, "Parasitic feed through cancellation techniques for enhanced electrical characterization of electrostatic microresonators ", *Sens Actuators A* 156 (2009), pp.36-42, 2009 .
- [5] S. A. Bhave, D. Gao, R. Maboudian and R. T. Howe, "Fully-differential poly-SiC Lamé-mode resonator and checkerboard filter," 18th IEEE International Conference on Micro Electro Mechanical Systems (MEMS 2005), Miami.
- [6] G. Wijeweera, B. Bahreyni, C. Shafai, A. Rajapakse, and D. Swatek, "Micro machined electric field sensor to measure ac and dc fields in power systems," *IEEE Trans. Power Del.*, vol. 24, no. 3, pp. 988–995, Jul. 2009.
- [7] C. M. N. Brigante, N. Abbate, A. Basile, A. C. Faulisi, and S. Sessa, "Towards miniaturization of a MEMS-based wearable motion capture system," *IEEE Trans. Ind. Electron.*, vol. 58, no. 8, pp. 3234–3241, Aug. 2011.
- [8] C. T.-C. Nguyen, "MEMS technology for timing and frequency control," *IEEE Trans. Ultrasonics Ferroelectr., Freq. Control*, vol. 54, no. 2, pp. 251–270, Feb. 2007.
- [9] M. Li, H. X. Tang, and M. L. Roukes, "Ultra-sensitive NEMS-based cantilevers for sensing, scanned probe and very high-frequency applications," *Nat. Nanotechnol.*, vol. 2, no. 2, pp. 114–120, Feb. 2007.
- [10] J. E.-Y. Lee and A. A. Seshia, "Parasitic feed through cancellation techniques for enhanced electrical characterization of electrostatic micro resonators," *Sens. Actuators A, Phys.*, vol. 156, no. 1, pp. 36–42, Nov. 2009.